Supplementary Information

For

Photosensitizer Cross-linked Nano-Micelle Platform for Multimodal Imaging Guided Synergistic Photothermal/Photodynamic Therapy

Xiaodong Liu‡[a], Guangbao Yang‡[b], Lifen Zhang[a], Zhuang Liu*[b], Zhenping Cheng*[a], Xiulin Zhu[a]

[a] *Suzhou key Laboratory of Macromolecular Design and Precision Synthesis, Jiangsu Key Laboratory of Advanced Functional Polymer Design and Application, Department of Polymer Science and Engineering, College of Chemistry, Chemical Engineering and Materials Science, Soochow University, Suzhou 215123, China.*

[b] *Institute of Functional Nano and Soft Materials (FUNSOM) and Jiangsu Key Laboratory for Carbon-Based Functional Materials and Devices, Soochow University, Suzhou 215123, China.*

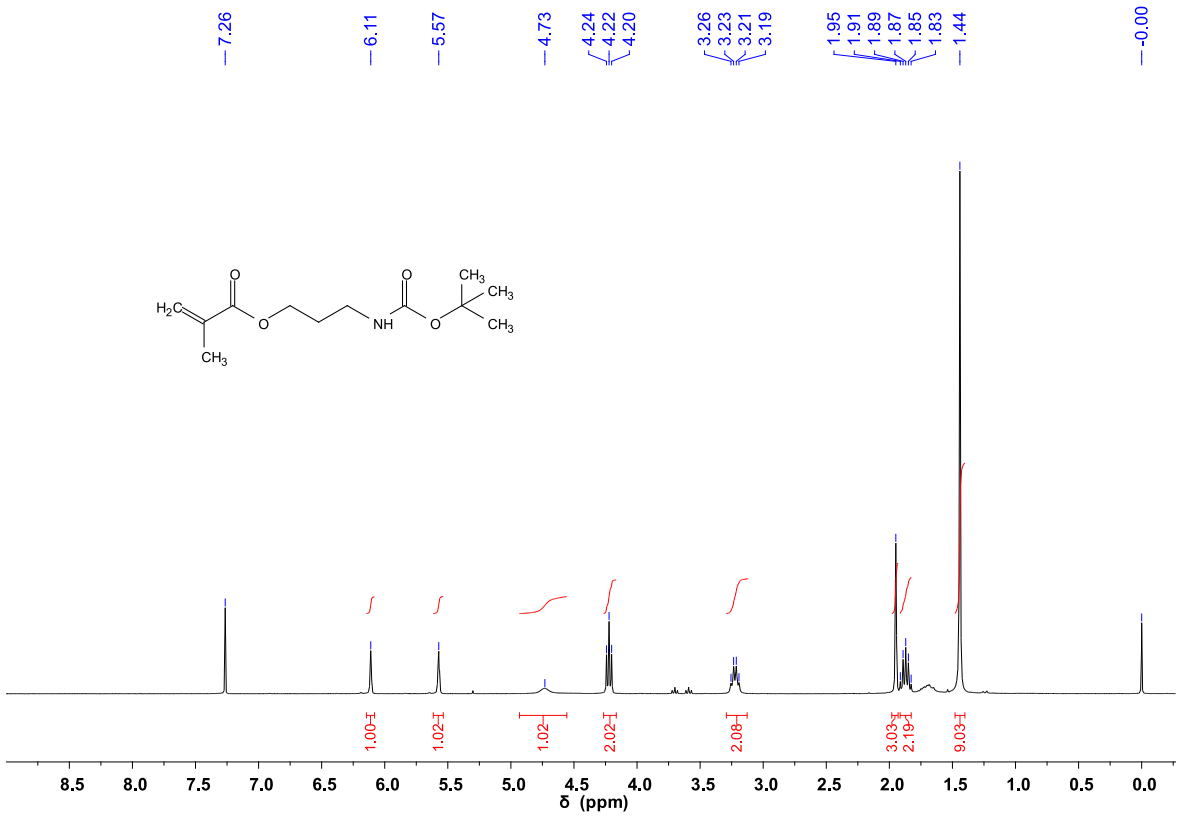

Figure S1. ^{1}H NMR spectrum of **BAPMA**.

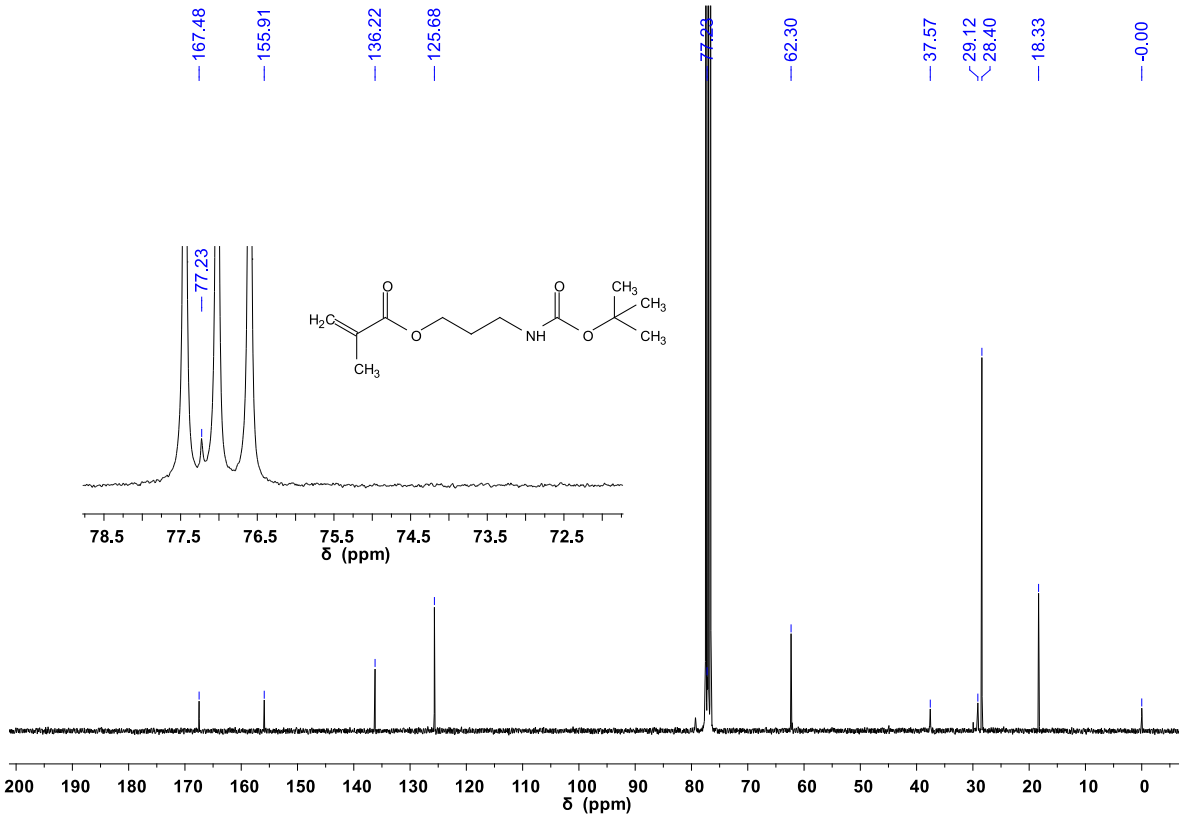

Figure S2. ^{13}C NMR spectrum of **BAPMA**.

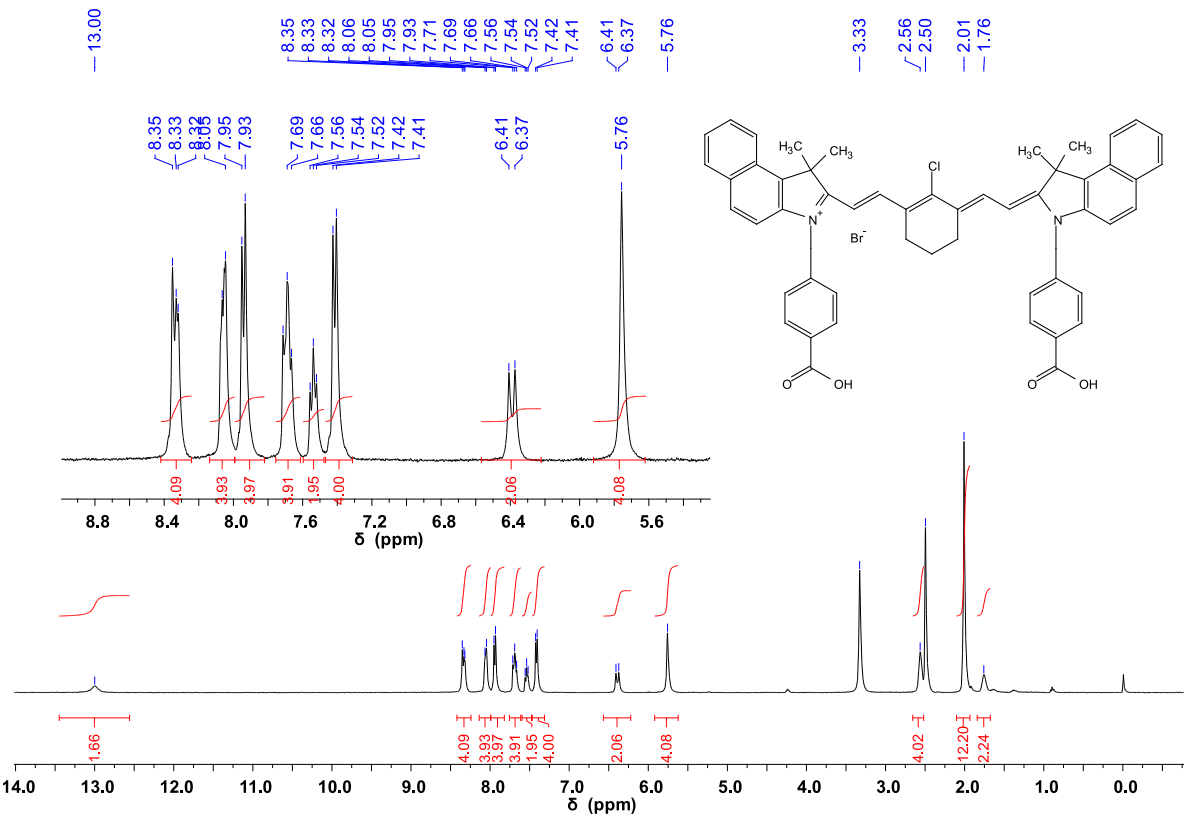

Figure S3. ^{1}H NMR spectrum of **IR825**.

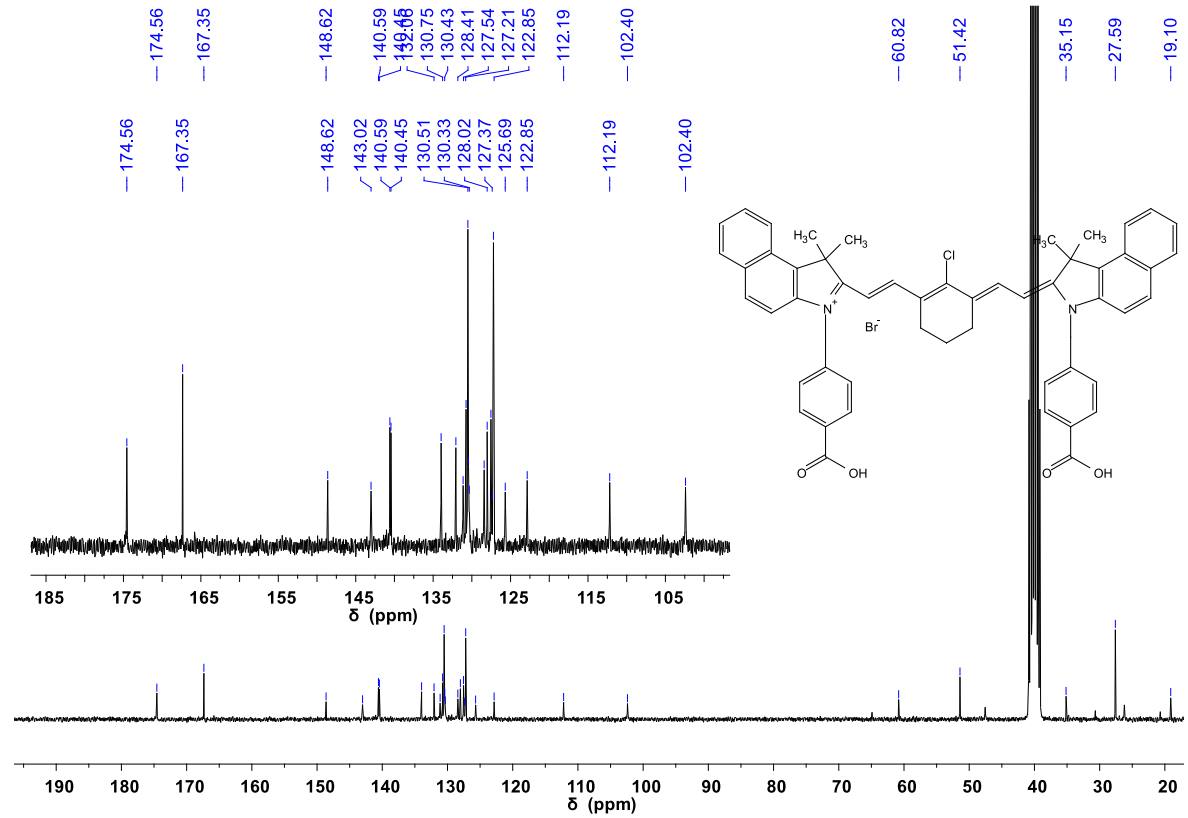

Figure S4. ^{13}C NMR spectrum of **IR825**.

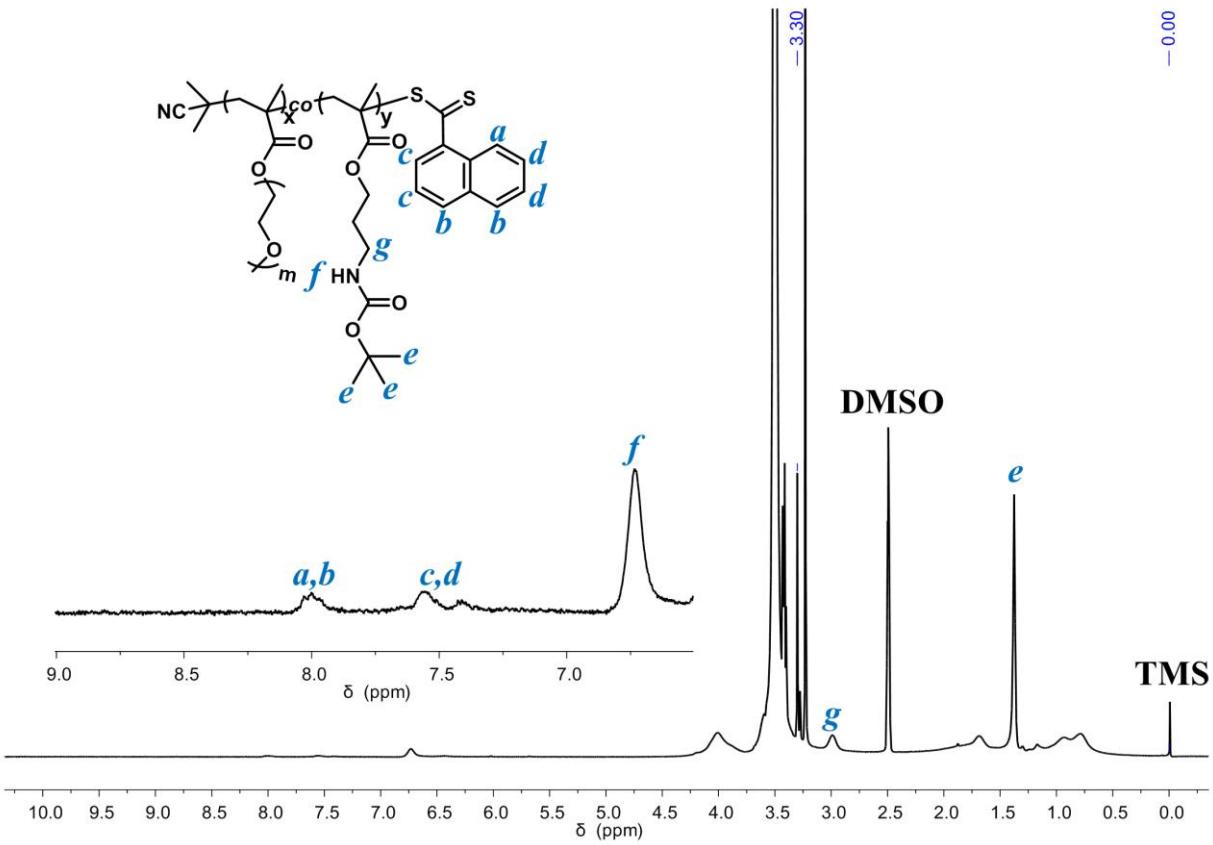

Figure S5. ^{1}H NMR spectrum of **P(PEGMA-*co*-BAPMA)** in DMSO-d_6.

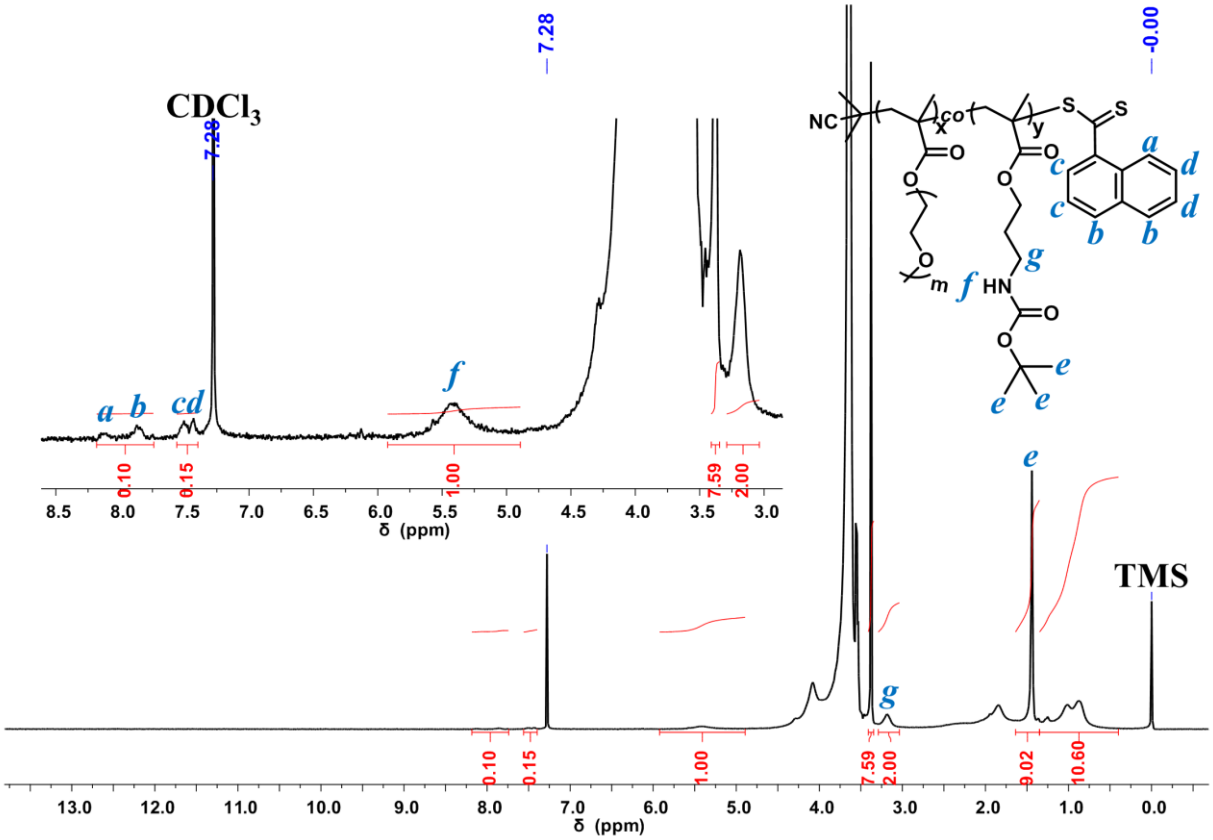

Figure S6. ^{1}H NMR spectrum of **P(PEGMA-*co*-BAPMA)** in $CDCl_3$.

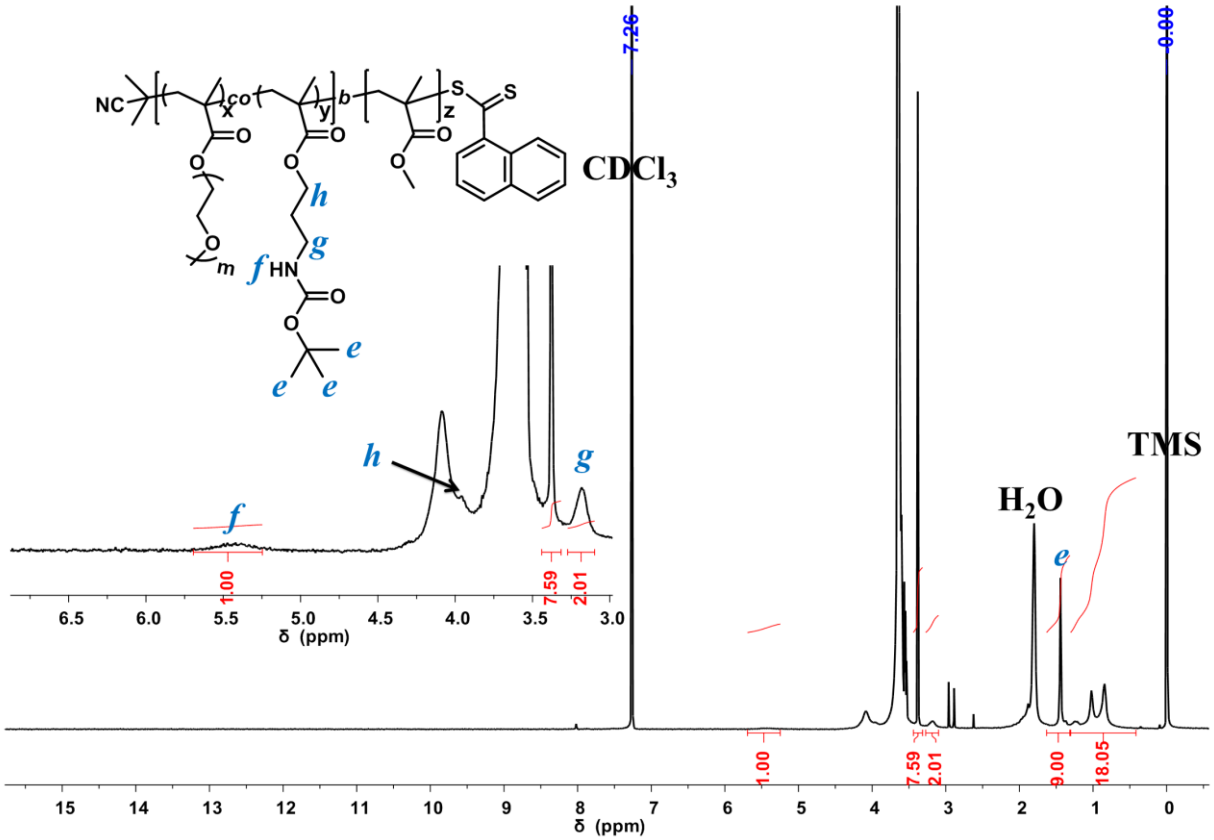

Figure S7. ^{1}H NMR spectrum of **P(PEGMA-*co*-BAPMA)-*b*-PMMA** in $CDCl_3$.

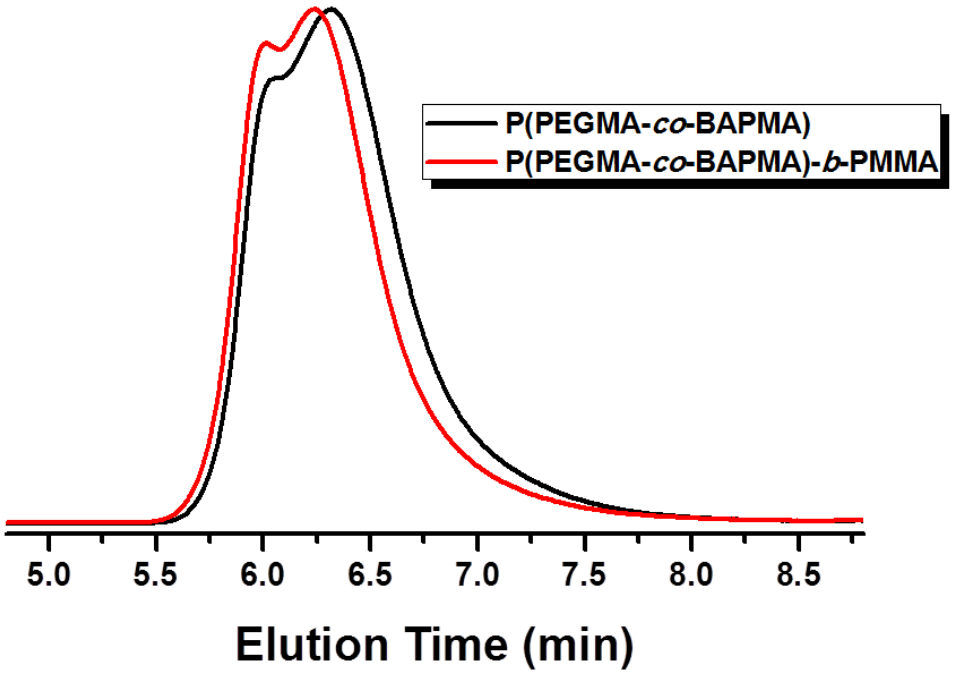

Figure S8. GPC elution curves of **P(PEGMA-*co*-BAPMA)** and **P(PEGMA-*co*-BAPMA)-*b*-PMMA**.

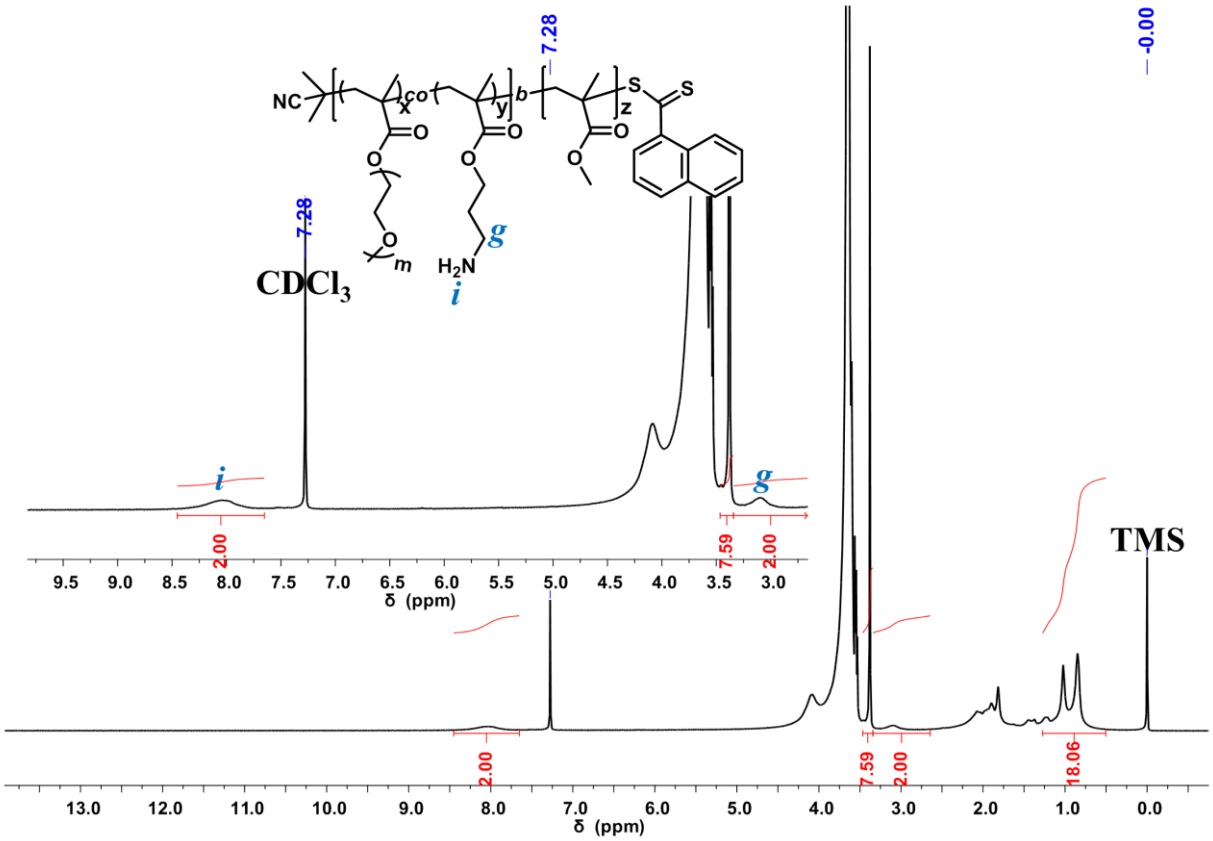

Figure S9. ^{1}H NMR spectrum of **P(PEGMA-*co*-APMA)-*b*-PMMA** in $CDCl_3$.

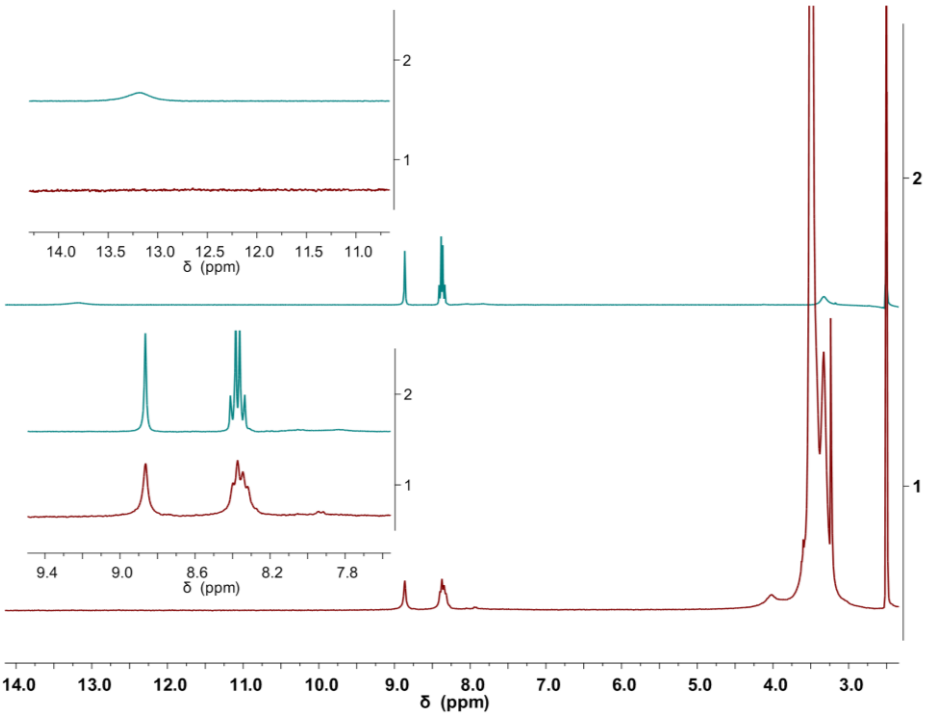

Figure S10. ^{1}H NMR spectral changes of **P(PEGMA-*co*-APMA)-*b*-PMMA** (in DMSO-d_6) before (**1**) and after (**2**) reaction with 5,10,15,20-tetrakis (4-carboxyphenyl) porphyrin (TCPP).

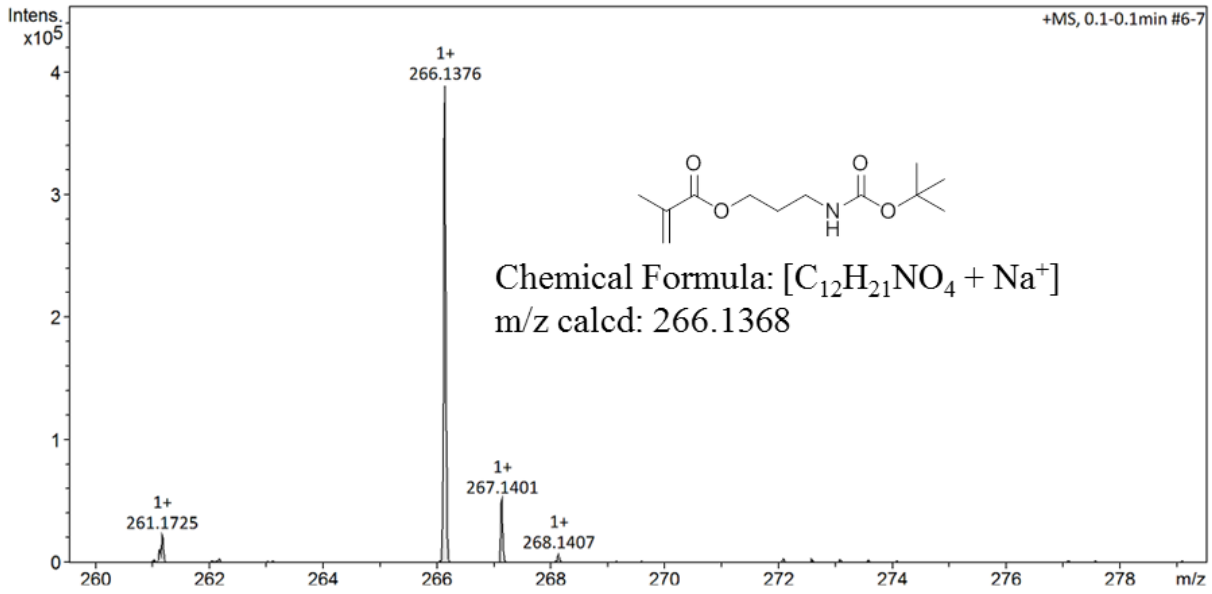

Figure S11. High resolution mass spectrum of **BABPA**.

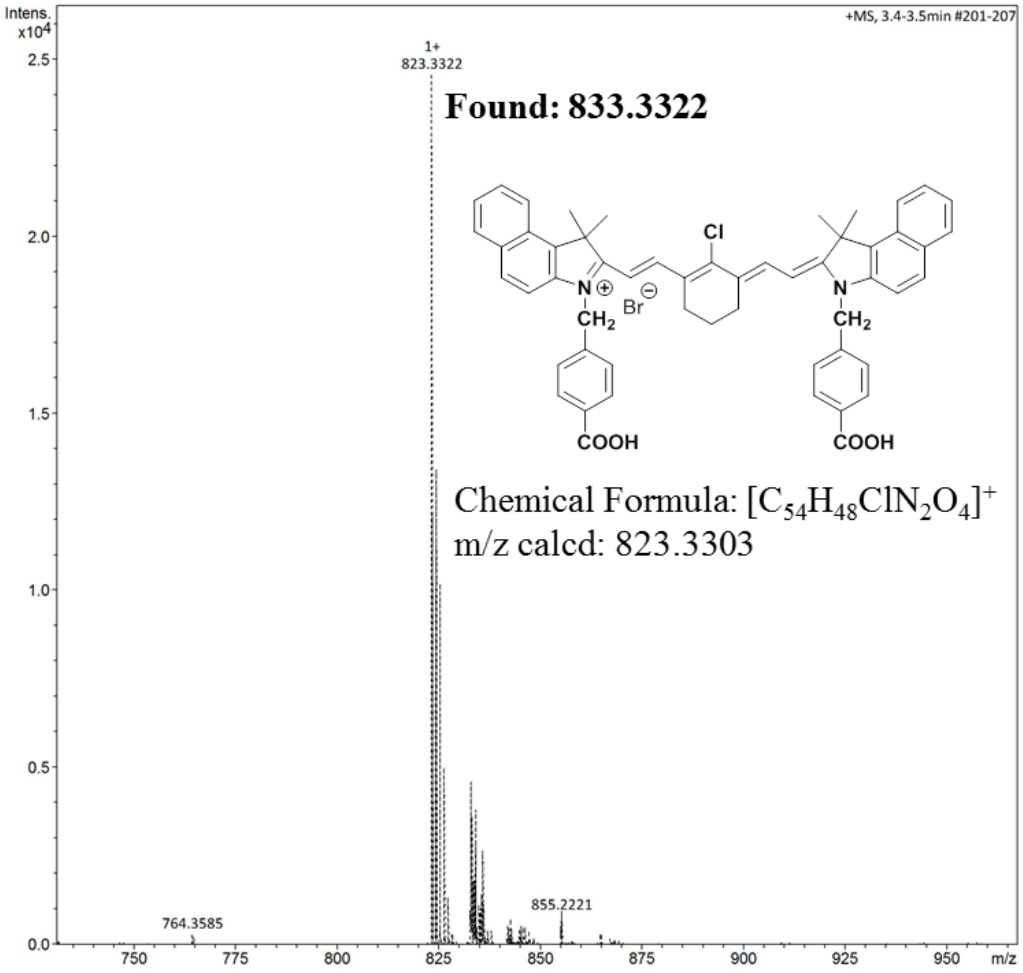

Figure S12. High resolution mass spectrum of **IR825**.

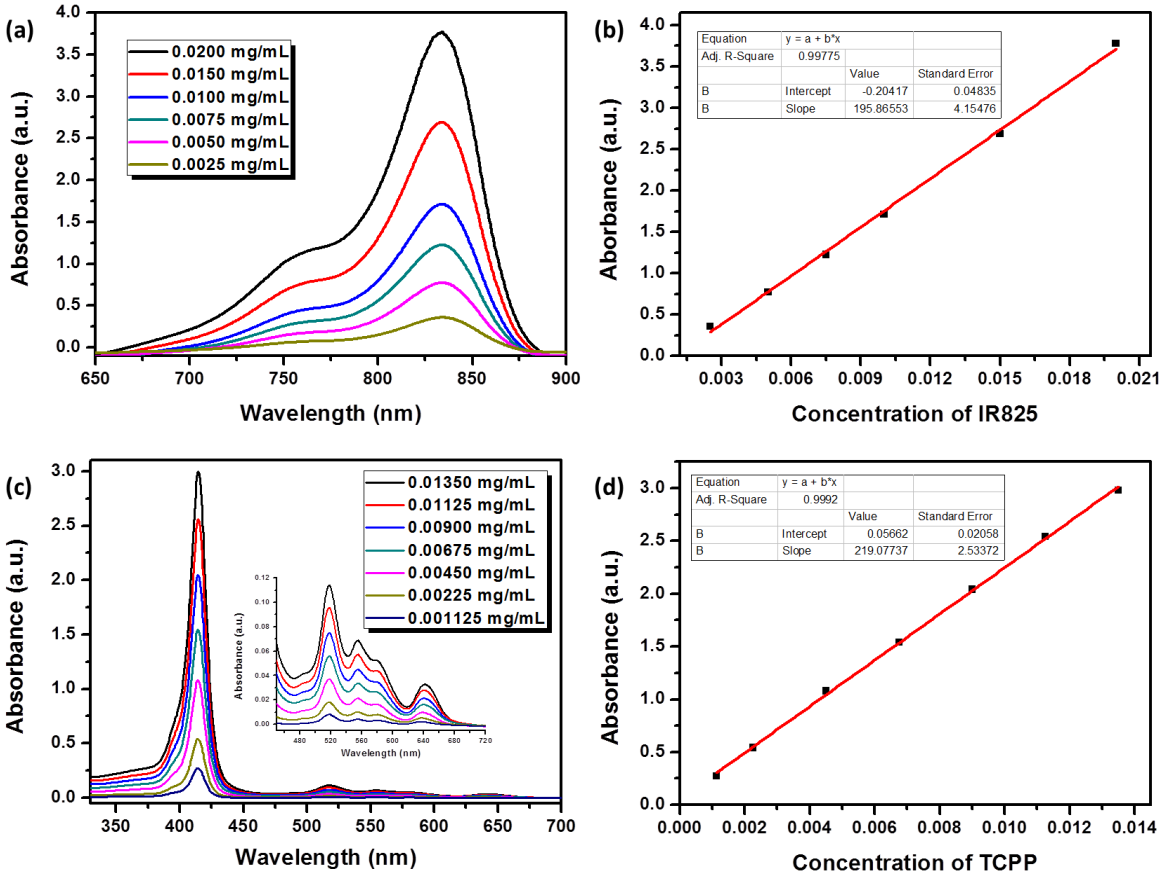

Figure S13. (a) Absorbance spectra of IR825 at different concentrations in DMF, (b) absorbance intensities of IR825 of different concentrations at 834 nm. (c) Absorbance spectra of TCPP at different concentrations in Na_2HPO_4-citric acid buffer solution (0.1 M, pH 8.5), (d) absorbance intensities of TCPP of different concentrations at 414 nm;

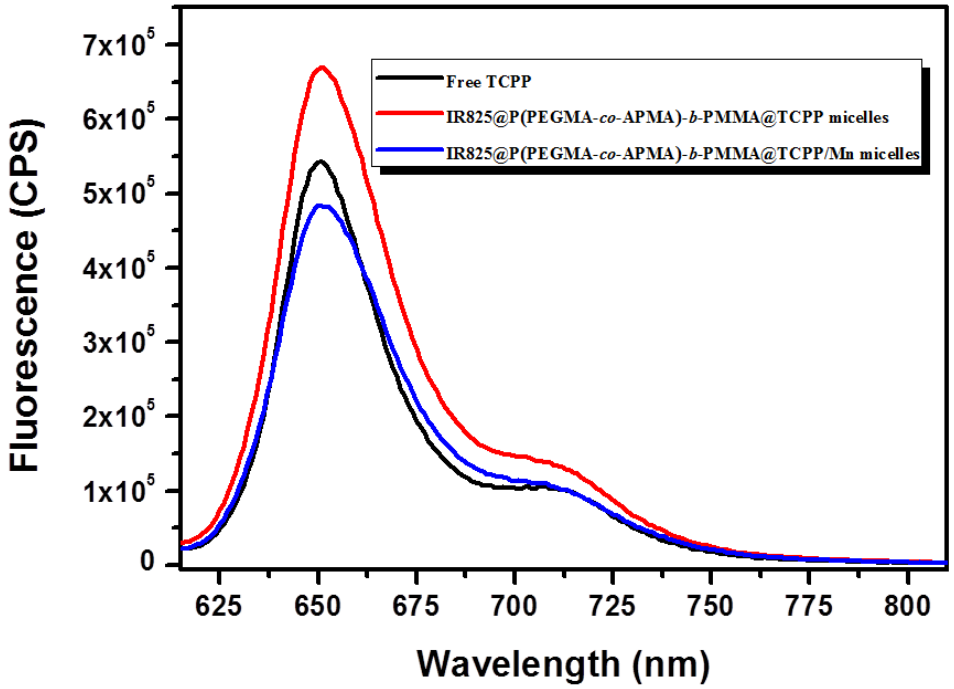

Figure S14. Fluorescence spectra of TCPP (in Na_2HPO_4-citric acid buffer solution, pH 8.5), IR825@P(PEGMA-*co*-APMA)-*b*-PMMA@TCPP micelles and IR825@P(PEGMA-*co*-APMA)-*b*-PMMA@TCPP/Mn micelles taken at the same TCPP concentration; λ_{em} = 600 nm.

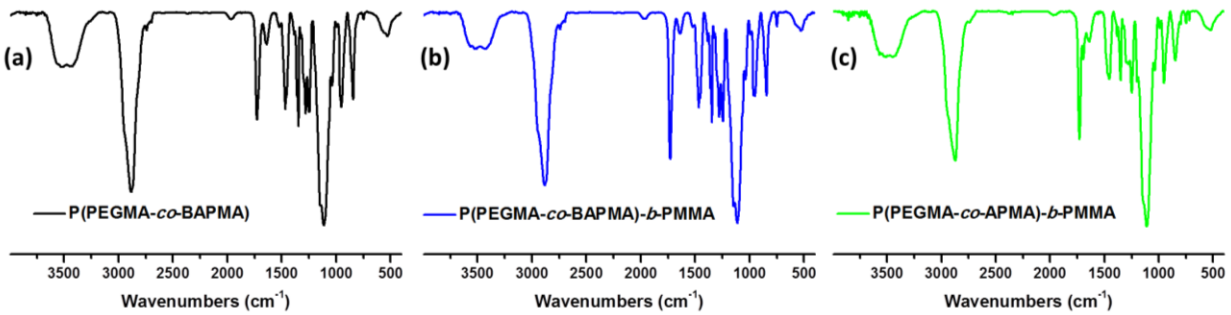

Figure S15. FT-IR spectra of (a) **P(PEGMA-*co*-BAPMA)**, (b) **P(PEGMA-*co*-BAPMA)-*b*-PMMA** and (c) **P(PEGMA-*co*-APMA)-*b*-PMMA**.

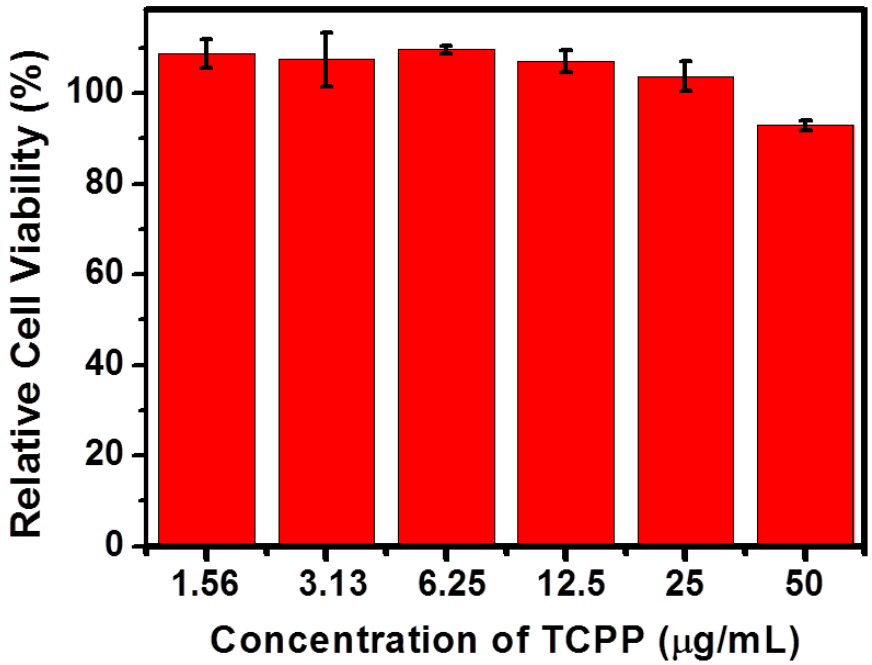

Figure S16. Relative viabilities of 4T1 cells after being incubated with different concentrations of free TCPP without light irradiation.

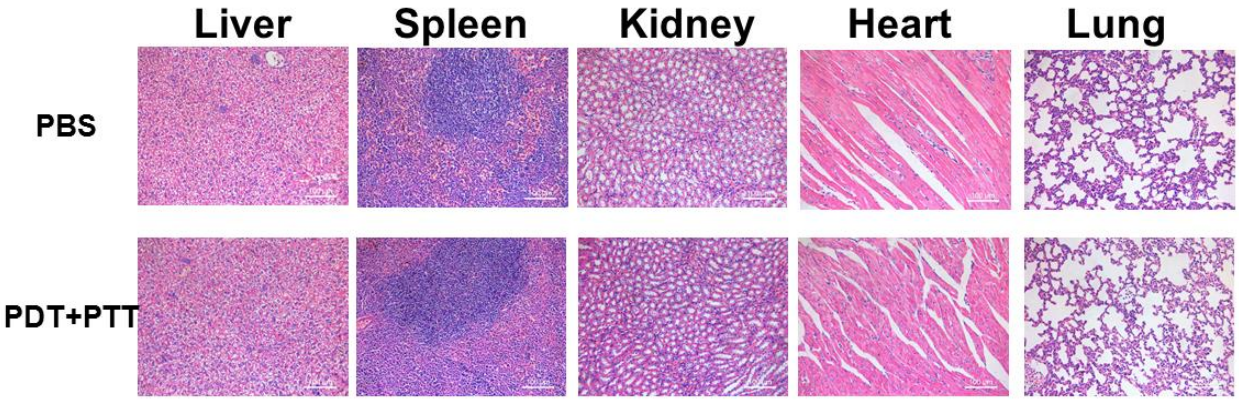

Figure S17. H&E stained images of major organs slices collected from untreated mice and mice 14 days post IR825@P(PEGMA-*co*-APMA)-*b*-PMMA@TCPP/Mn micelles injection and then photothermal and photodynamic treatment.